

# Indirect Signals from Dark Matter in Split Supersymmetry

Asimina Arvanitaki and Peter W. Graham

Institute for Theoretical Physics

Department of Physics

Stanford University

Stanford, CA 94305 USA

email: aarvan@stanford.edu, pwgraham@stanford.edu

## Abstract

We study the possibilities for the indirect detection of dark matter in Split Supersymmetry from  $\gamma$ -rays, positrons, and anti-protons. The most promising signal is the  $\gamma$ -ray line, which may be observable at the next generation of detectors. For certain halo profiles and a high mass neutralino, the line can even be visible in current experiments. The continuous  $\gamma$ -ray signal may be observable, if there is a central spike in the galactic halo density. The signals are found to be similar to those in MSSM models. These indirect signals complement other experiments, being most easily observable for regions of parameter space, such as heavy wino and higgsino dominated neutralinos, which are least accessible with direct detection and accelerator searches.

## 1 Introduction

The principle of naturalness seems to fail in explaining the small size of the cosmological constant. The apparent fine-tuning required dwarfs that of the gauge hierarchy problem. Further, the current experimental bound on the Higgs mass requires a 1% tuning in the MSSM [1], the most popular solution to the gauge hierarchy problem. In view of these problems with naturalness, Arkani-Hamed and Dimopoulos have proposed accepting a single fine-tuning in the Higgs sector [2].

In exchange, many of the problems of the MSSM, including the SUSY flavor and CP problems and the long lifetime of the proton, are easily solved within one framework without sacrificing either gauge coupling unification or the natural dark matter candidate of the MSSM. This model, called Split Supersymmetry [3], breaks SUSY at an intermediate scale,  $M_S$ , between the weak and Planck scales, giving the squarks and sleptons masses  $\sim M_S$ . An approximate R-symmetry keeps the gauginos and higgsinos light, around a TeV in mass [4]. This scale is chosen to give a dark matter candidate whose relic abundance can be in the observed range [5] and to preserve gauge coupling unification.

Since dark matter is one of the main motivations for and constraints on Split SUSY, it is important to understand the nature of the dark matter candidate. We will assume that the neutralino is the LSP. The relic abundance and direct detection signals have already been calculated [3, 6]. We build on that work to study indirect detection signals from the annihilation of neutralinos in the dark matter halo of our galaxy. These annihilations produce cosmic rays which could be used not only to discover dark matter but also to determine some of its properties. We study the annihilation signals from  $\gamma$ -rays, positrons, and antiprotons in Split SUSY. For  $\gamma$ -rays, we calculate the fluxes from the center of the galaxy where the neutralino density is greatest. Many processes contribute to the continuous flux of these cosmic rays at tree level. There are also one loop diagrams which mediate the processes  $\chi^0\chi^0 \rightarrow \gamma\gamma$  and  $\chi^0\chi^0 \rightarrow \gamma Z$ , creating two sharp lines in the  $\gamma$ -ray spectrum [7]. The width of these lines is set by the kinetic energy distribution of the dark matter particles, since photons propagate through the galaxy without significant diffusion. The energy of these lines then serves as a very precise measure of the mass of the dark matter particle.

We find that cosmic ray signals from neutralino annihilations in Split SUSY are similar to those in many MSSM models. The lines in the  $\gamma$ -ray spectrum should be detectable by future experiments, if not by current ones. The continuous  $\gamma$ -ray signal is visible for dark matter density profiles with a spike at the galactic center. Positrons and antiprotons from neutralino annihilations are more challenging, as they can be observed only if the backgrounds are well understood. The prospects for indirect detection are generally promising and best in areas where collider and direct detection searches are difficult.

## 2 Indirect signals

### 2.1 Split Supersymmetry framework

To find the flux of cosmic rays from neutralino annihilations in the halo, we must first find the cross sections for all the neutralino annihilation processes. Certain differences between Split SUSY and the MSSM are crucial to this analysis. The most salient is the lack of scalar superpartners at low energies. The tree level Lagrangian in Split SUSY below the SUSY breaking scale,  $M_S$ , contains the terms

$$\mathcal{L} \supset \tilde{B}(\kappa'_1 h^\dagger \tilde{H}_1 + \kappa'_2 h \tilde{H}_2) + \tilde{W}^a(\kappa_1 h^\dagger \tau^a \tilde{H}_1 + \kappa_2 \tilde{H}_2 \tau^a h) - \lambda |h|^4 - \mu \tilde{H}_1 \tilde{H}_2 - \frac{1}{2}(M_1 \tilde{B} \tilde{B} + M_2 \tilde{W} \tilde{W} + M_3 \tilde{g} \tilde{g}).$$

The neutralino and chargino mass matrices from this Lagrangian are:

$$\mathbf{M}_{\chi^0} = \begin{pmatrix} M_1 & 0 & -\frac{\kappa'_1 v}{\sqrt{2}} & \frac{\kappa'_2 v}{\sqrt{2}} \\ 0 & M_2 & \frac{\kappa_2 v}{\sqrt{8}} & -\frac{\kappa_1 v}{\sqrt{8}} \\ -\frac{\kappa'_2 v}{\sqrt{2}} & \frac{\kappa_2 v}{\sqrt{8}} & 0 & -\mu \\ \frac{\kappa'_1 v}{\sqrt{2}} & -\frac{\kappa_1 v}{\sqrt{8}} & -\mu & 0 \end{pmatrix},$$

$$\mathbf{M}_{\chi^\pm} = \begin{pmatrix} M_2 & \frac{\kappa_1 v}{2} \\ \frac{\kappa_2 v}{2} & \mu \end{pmatrix},$$

with  $v = 246$  GeV. At  $M_S$  the following supersymmetric relations are satisfied:

$$\kappa'_1 = \sqrt{\frac{3}{10}} g_1 \sin \beta \quad \kappa'_2 = \sqrt{\frac{3}{10}} g_1 \cos \beta \quad \kappa_1 = \sqrt{2} g_2 \sin \beta \quad \kappa_2 = \sqrt{2} g_2 \cos \beta \quad \lambda = \frac{\frac{3}{5} g_1^2 + g_2^2}{8} \cos^2 2\beta.$$

These couplings must be run from their SUSY values at  $M_S$  down to the scale at which we are working. This affects all the couplings and crucially raises the Higgs mass as high as 160 to 170 GeV [2, 8, 9], increasing the Higgs width to around 1 GeV. The lack of scalar superpartners greatly decreases the number of parameters from the MSSM. Split SUSY models are specified completely in terms of the input parameters  $M_S$ ,  $\tan \beta$ ,  $\mu$ , and the gaugino masses.

### 2.2 Calculation of annihilation rates

The DarkSUSY package calculates the current relic abundance of the lightest neutralino, the cross sections for direct detection, and the flux of cosmic rays from neutralino annihilation in the halo [10]. Our calculations are based on this package as modified in [6] to include the running of the couplings from the SUSY breaking scale, the absence of scalar superpartners, and the effect of the process  $\chi^0 \chi^0 \rightarrow h \rightarrow WW^*$  on the relic abundance.

DarkSUSY only calculates the neutralino annihilation rate into two body final states. The average decay products of these two on-shell particles are then added together to produce the indirect signal. Normally these channels are the dominant contribution to the annihilation rate, but since the Higgs has a large mass and width, there is a region where the neutralinos can annihilate resonantly through an s-channel Higgs. Even if its energy is below threshold for  $WW$  production, a Higgs heavier than 130 GeV has a large branching ratio for decays to  $WW^*$ , which is not a two-body final state since one of the  $W$ 's is not on-shell. When it is on resonance, this process can dominate the neutralino annihilation rate and significantly affect the relic abundance.

It is necessary to include the effects of this annihilation channel,  $\chi^0 \chi^0 \rightarrow h \rightarrow WW^*$ , in the calculation of indirect signals as well. However, it is suppressed by the low velocity of the neutralinos at the present time. In the zero velocity limit they have no angular momentum and can only create a pseudoscalar state in the s-channel, not a scalar. Because of the Higgs resonance, a velocity-suppressed signal could still be significant. We use the known rate for the process  $h \rightarrow WW^* \rightarrow W f \bar{f}$ , where  $f$  is any SM fermion [11]. The usual DarkSUSY routines are then used to find the average decay products of the fermions, ignoring the complication that the center of mass frame of the fermions, the  $W^*$  frame, is moving. Taking the motion into account would slightly affect the energies of the decay products, but is unnecessary since we merely wish to be sure this channel is negligible below threshold for

WW production. We find that the velocity suppression wins and the Higgs resonance channel contributes very little to the annihilation signals at the present time. In principle, the usual DarkSUSY calculation also fails for channels with a Higgs in the two body final state, however we find that these processes are negligible as well.

### 2.3 Halo model

The density profile of the galactic dark matter halo can affect the calculated indirect signals greatly. We take the Burkert profile [12]:

$$\rho(r) = \frac{\rho_0}{(1 + \frac{r}{R})(1 + \frac{r^2}{R^2})} \quad (1)$$

where  $\rho_0 = 0.839 \frac{\text{GeV}}{\text{cm}^3}$  and  $R = 11.7$  kpc. This is a conservative profile from the point of view of annihilation signals, since it does not have a spike at the center of the galaxy. Other halo profiles are commonly parameterized as:

$$\rho(r) = \frac{\rho_0}{(\frac{r}{R})^\gamma (1 + (\frac{r}{R})^\alpha)^{\frac{(\beta-\gamma)}{\alpha}}}. \quad (2)$$

These do have a spike in the center of the galaxy for positive  $\gamma$ . We will consider the Navarro-Frenk-White (NFW) model [13] with  $\alpha = 1$ ,  $\beta = 3$ , and  $\gamma = 1$  as an alternative to the conservative Burkert profile. We hold fixed the density at the radius of the solar system and so take  $R = 20$  kpc and  $\rho_0 = 0.235 \frac{\text{GeV}}{\text{cm}^3}$ . This model will tend to produce greater annihilation signals, since they are proportional to the square of the density. In the following sections we will compare the results for the Burkert and NFW profiles in detail.

## 3 $\gamma$ -ray, positron and antiproton signals

In Fig. 1 we plot the points in parameter space that satisfy the current experimental bounds on the relic abundance ( $0.094 < \Omega h^2 < 0.129$ ) from WMAP [14]. We have chosen  $\tan \beta = 5$  and  $M_S = 10^9$  GeV with  $\frac{M_2}{M_1} = 2$ . For low values of  $M_1$ , there is a region where the neutralino annihilates through an s-channel Higgs resonance. The neutralino in this region is almost purely bino. Away from the Higgs resonance and as the mass of the neutralino increases following the diagonal line, the content of the neutralino switches from bino to higgsino. For  $m_\chi > 1$  TeV, the line turns upwards and the neutralino becomes almost purely higgsino. A wino dominated LSP can only be found at values of  $M_1$  and  $\mu$  larger than 3 TeV with  $\frac{M_2}{M_1} < 1$ , resulting in a high mass neutralino. It should be noted that the above results are consistent with [6].

In order to compare the continuous spectra of antiprotons, positrons, and  $\gamma$ -rays in this framework with the cosmic ray background, we consider four characteristic points in parameter space. We calculate the fluxes for a bino, wino, and higgsino dominated neutralino, as well as a neutralino that corresponds to the Higgs resonance region. The masses and compositions of the LSPs are given in Table 1.

	$M_1(\text{GeV})$	$M_2(\text{GeV})$	$\mu(\text{GeV})$	$m_\chi(\text{GeV})$	$\tilde{B}$ fraction	$\tilde{W}$ fraction	$\tilde{H}$ fraction	$\Omega h^2$
bino	300	600	350	281	0.730	0.010	0.260	0.111
higgsino	1400	2800	1200	1192	0.024	0.002	0.974	0.109
wino	4400	2200	3500	2197	$\sim 10^{-7}$	0.997	0.003	0.099
higgs resonance	75.5	151	250	69.8	0.922	0.019	0.059	0.122

Table 1: The characteristic bino, wino, higgsino and higgs resonance points. The mass, composition, and relic abundance of the LSP is shown for each point. For all points  $\tan \beta = 5$  and  $M_S = 10^9$  GeV.

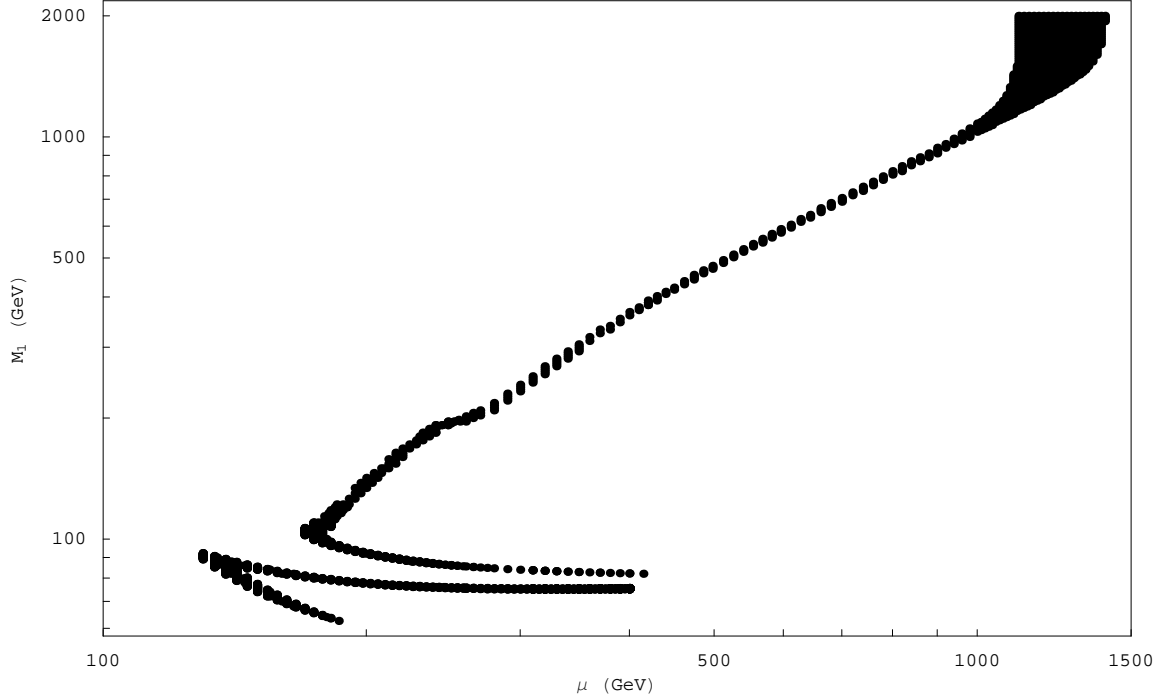


Figure 1: Points in the  $\mu - M_1$  plane with relic abundance within the WMAP allowed range. Here  $M_S = 10^9$  GeV,  $\tan\beta = 5$ , and  $M_2 = 2M_1$ . The horizontal lines at low  $M_1$  are the Higgs resonance region.

### 3.1 $\gamma$ lines

The annihilations of two neutralinos to two  $\gamma$ -rays or to a  $\gamma$  and a  $Z$  produce lines in the  $\gamma$ -ray spectrum which can provide a striking signature of the dark matter particle. The energy of the  $\gamma\gamma$  line is  $E_\gamma = m_\chi$ , since the neutralinos have low velocities. The  $\gamma Z$  line occurs at an energy  $E_\gamma = m_\chi - \frac{m_Z^2}{4m_\chi}$ . This is practically indistinguishable from the  $\gamma\gamma$  line for large neutralino masses, where the two will be easily within any current experiment's energy bin size.

Unlike positrons and antiprotons,  $\gamma$ -rays can travel through the halo with little diffusion, especially if they are highly energetic. This makes probing distant sources that have increased local density, such as the center of the galaxy, possible. Now, the halo profile chosen for our calculations starts to play an important role. As already discussed, many halo models favor the existence of a spike in the dark matter profile at the galactic center. We calculate the flux from this direction in the sky averaged over a solid angle of  $10^{-5}$  sr, which we assume to be the angular resolution of our detector.

Fig. 2 shows the expected flux of the two  $\gamma$  lines from the direction of the galactic center as a function of the neutralino mass, for all the points shown in Fig. 1. It also includes a scan of wino-dominated neutralinos (the strip on the right) with the same parameters except  $M_1 = 2M_2$ . Here we have used the NFW profile. For the Burkert profile the signals are reduced by a factor of about 1000. The Higgs resonance causes a significant suppression of the signal at  $m_\chi \approx \frac{1}{2}m_H \approx 80$  GeV. The  $\gamma$  line signals are peaked at  $\approx 3 \times 10^{-14}$   $\text{cm}^{-2}\text{s}^{-1}$ . This signal is not observable by space-based experiments, since even GLAST, with an effective area of  $\sim 10^4$   $\text{cm}^2$  [15], will see only  $\sim 0.01$  photons  $\text{yr}^{-1}$  from the galactic center and  $\sim 1$  photons  $\text{yr}^{-1}$  from the entire galaxy. Ground based telescopes, such as HESS [16], have a much larger effective area ( $\sim 10^8$   $\text{cm}^2$ ), allowing a possible detection of the signal.

Of course, the astrophysical background could also overwhelm the signal, though a line will be much easier to

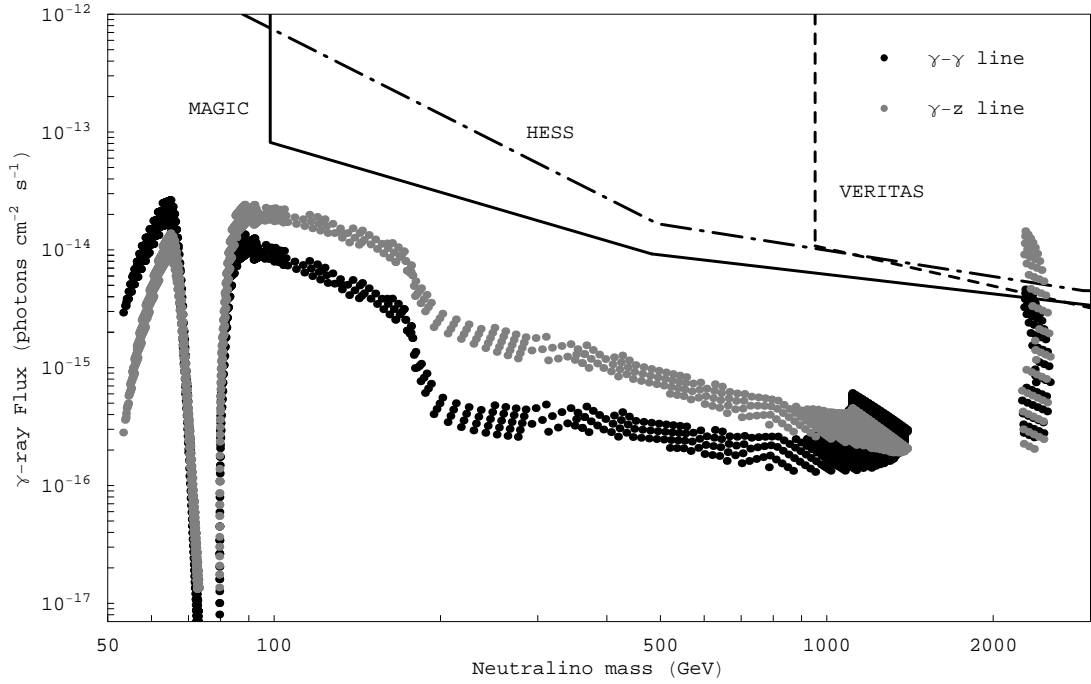


Figure 2: The strength of the gamma lines from  $\chi^0\chi^0 \rightarrow \gamma\gamma$  and  $\chi^0\chi^0 \rightarrow \gamma Z$  is plotted against neutralino mass for the points in Fig. 1 and for a scan of wino-dominated LSPs with  $M_1 = 2M_2$  (section on right). The flux is averaged over a  $10^{-5}sr$  cone around the direction of the center of the galaxy. The sensitivities of three current experiments are shown. We have used the NFW profile for the signal. While the energy of the  $\gamma\gamma$  line is equal to  $m_\chi$ , the energy of the  $\gamma Z$  line is somewhat smaller. The suppression due to the Higgs resonance is clearly visible.

detect than the continuous spectrum. Fig. 2 includes the sensitivities of three currently operating telescopes. These sensitivities are calculated for a 1 year exposure from the known integral point source sensitivities [15, 17]. We expect the actual sensitivity to be better because our signal is not just a point source but also a monochromatic line which aids in distinguishing it from the background. However, the quoted sensitivity should be approximately correct because the background falls sharply with energy. If a line source is observable above the background at its own energy, it is probably observable above the total integrated background greater than its energy. Further, a calculation of the sensitivity to a line source [18] gives a sensitivity for HESS and VERITAS which is very similar to the quoted sensitivities. From Fig. 2 it is clear that MAGIC has the best sensitivity in the relevant energy range although HESS is quite similar and VERITAS is just as sensitive above 1 TeV. HESS and VERITAS are similar air-Cherenkov telescopes, but VERITAS is in the northern hemisphere. Since the galactic center is a southern source, VERITAS observes it at a high zenith angle giving a higher energy threshold, but better sensitivity.

For high mass neutralinos the signal remains roughly constant, in contrast to the background which falls as a power law as in Fig. 3. Unfortunately, the detectors have large energy resolutions, around 10-25%, which must be factored in when comparing the signal in Fig. 2 to the background, making it harder to see a line. For the NFW profile many of the heavier wino-dominated points should be visible at current experiments, especially since the  $\gamma - \gamma$

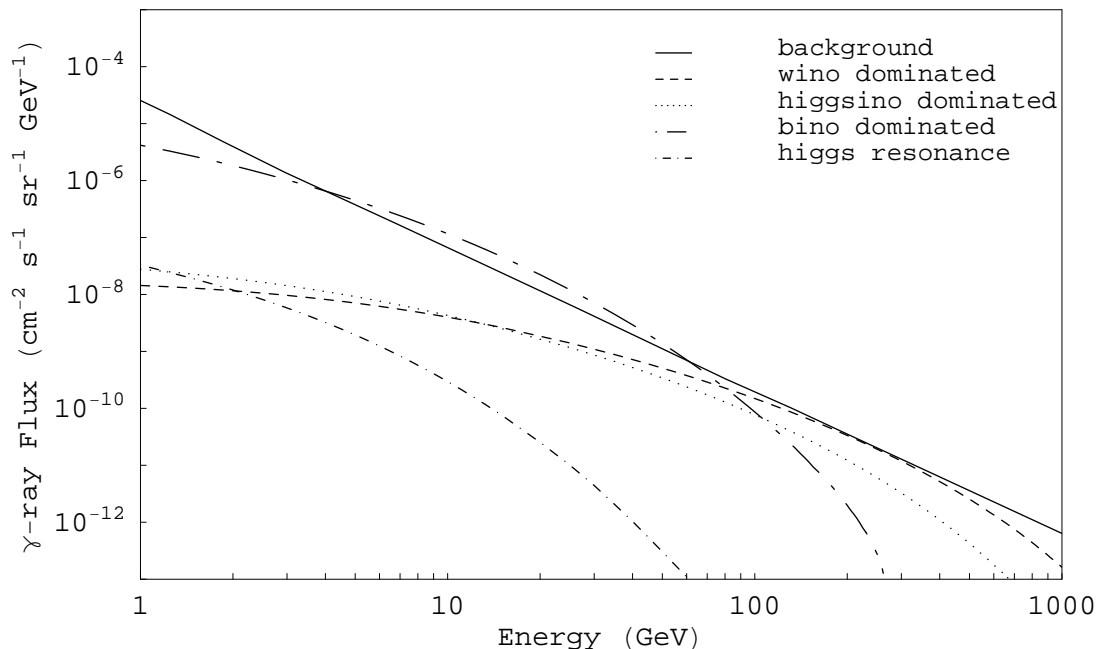


Figure 3: The continuous gamma ray spectra from the galactic center for the four characteristic points and the expected background. We have used the less conservative NFW profile for the signals.

and  $\gamma$ -Z signals should be added together as they will not be distinguishable in current telescopes. The rest of the points are almost visible and will be probed by next generation experiments. In addition, since there are multiple experiments operating in this energy range, a discovery could be confirmed easily. Of course, these results depend strongly on the halo profile and so the improvements in sensitivity of future telescopes will really be allowing us to probe halo profiles with less dark matter at the center of the galaxy.

Using the Burkert profile reduces the signal from the galactic center by a factor of 1000 making it probably undetectable at current or next generation telescopes. In this case it would actually be much easier to observe the signal by observing the entire galaxy instead of just the center because the density is roughly constant over the galaxy. Thus telescopes like GLAST with a large field of view have an advantage over telescopes which must be focused on a small portion of the sky. Since GLAST will see at most  $\sim 1$  photon  $\text{yr}^{-1}$  in the  $\gamma$ -line for either the Burkert or NFW profiles, it is probably not enough for a detection. But because this is about the expected level of the background for neutralinos with mass  $\gtrsim 1$  TeV, a similar next generation telescope might even be able to detect the line signal in the case of a halo profile without a spike at the galactic center.

The calculated  $\gamma$  line signals are similar in strength to those of MSSM models, being slightly smaller than the signal from Anomaly Mediated SUSY Breaking (AMSB) models but larger than that from mSUGRA models [19]. In AMSB models the LSP is either wino or higgsino dominated and so the comparison should be with those points. The mSUGRA models can also have a bino LSP and allow a general comparison with Split SUSY. The new feature in Split SUSY is the Higgs resonance region where the flux is greatly suppressed. Away from this region, the prospects

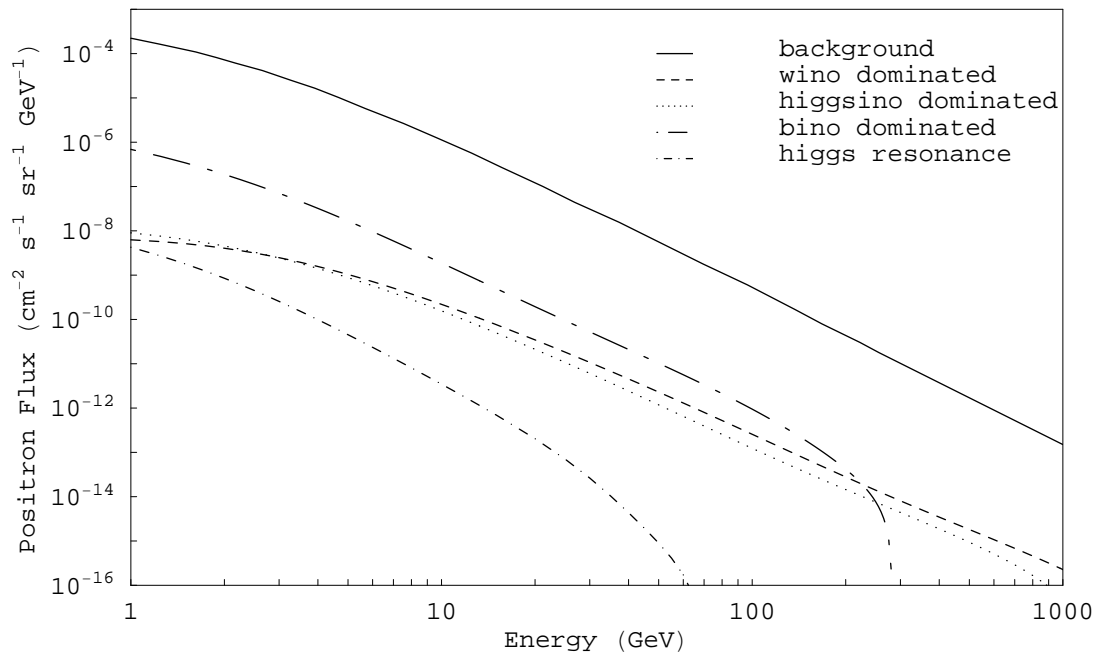


Figure 4: The continuous positron spectra for the four characteristic points and the expected background. We have used the NFW profile though it will not affect the signals greatly, since they depend primarily on the local halo density.

for the detection of the  $\gamma$  line in Split SUSY are much the same as in the MSSM.

### 3.2 Continuous $\gamma$ -ray, antiproton and positron flux

The continuous spectrum of  $\gamma$ -rays, antiprotons and positrons is mainly produced from the decay of annihilation products and, in particular for  $\gamma$ -rays, the radiative emission of photons when those annihilation products propagate through the halo. While  $\gamma$ -rays make it possible to probe the galactic center directly, charged antimatter can only propagate a few kpc, and the signal will be determined by the known local halo density.

In Figs. 3, 4, and 5, we present the differential yields for the four characteristic points, as evaluated using the NFW profile. We have used the solar modulation routines in DarkSUSY to account for the propagation of antimatter in our solar system. In the Higgs resonance region the signal is strongly suppressed, as expected, because the LSP is almost purely bino and has reduced coupling strength. The signals from all other points are comparable in comparison to the background, merely shifted towards higher energies for the higher mass LSPs. The flux goes to zero as the energy approaches  $m_\chi$ . Even though the number of tree level diagrams contributing to the yield is reduced by the absence of the scalar superpartners, the calculated signal is not much smaller than in ordinary SUSY models [20, 21, 22]. LSP annihilations in an AMSB model provide a slightly larger signal.

The calculated signal for the  $\gamma$ -ray spectrum with the NFW profile is comparable to the background while the

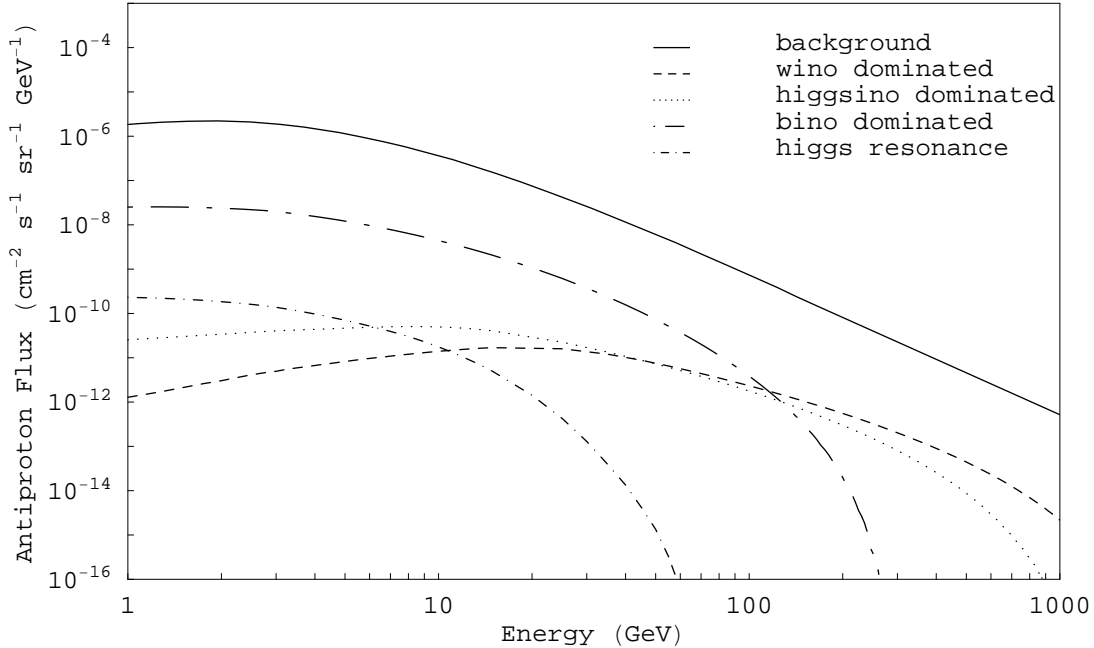


Figure 5: The continuous antiproton spectra for the four characteristic points and the expected background. We have used the NFW profile though it will not affect the signals greatly, since they depend primarily on the local halo density.

antimatter signals are at least two orders of magnitude smaller than their backgrounds [15, 23, 24, 25]. For  $\gamma$ -rays, this signal should be observable by both ground and space based telescopes. The signal is suppressed without a spike in the density at the galactic center. For the Burkert profile, this suppression translates to a factor of  $\sim 10^{-3}$ . This signal is below the statistical errors for the background and so unobservable for experiments like GLAST and at experimental sensitivity for ground based telescopes like VERITAS. For antiprotons and positrons, the signal cannot be conclusively observed by current or next generation experiments. Since charged antimatter particles cannot reach us from the center of the galaxy, the calculated fluxes will not be affected by the presence or absence of a cusp.

To determine whether these signals are observable, it is also important to understand the background model. There is a lot of uncertainty about the interstellar medium in which the diffuse  $\gamma$ -ray background and antimatter particles propagate. There have been efforts to create a viable model that agrees with the latest data [26]. More data from current and next generation experiments can improve our understanding of the background spectrum. In the absence of a well understood background model, it may be impossible to see a continuous  $\gamma$ -ray or antimatter signal that is a couple orders of magnitude below background, even if it is above the statistical error.

Although the spectrum produced is similar in shape to the background there are several features which should allow a detection. The annihilation signal has a characteristic rise compared to the background and then decreases abruptly at the neutralino mass. If there is a central spike in the density profile, the  $\gamma$ -ray signal should be readily observable. With a good enough understanding of the background, even the antimatter or the  $\gamma$ -ray signal from the



Burkert profile could be observable.

## 4 Conclusion

We have discussed the basic aspects of indirect dark matter signals in the Split SUSY scenario. In general, the situation is similar to that in the MSSM, though with more restrictions on the possible models. The positron and antiproton spectra probably cannot be detected due to the large uncertainty in the background and the low annihilation signal produced. The continuous  $\gamma$ -ray signal will be difficult to observe for conservative halo profiles. However, a central spike in the galactic halo density could make this signal observable at current or near-future detectors.

The  $\gamma$ -ray lines are easier to detect than the continuous spectra, since there are no other known sources for such a signal. Current experiments can already probe certain regions of Split SUSY parameter space with a less conservative halo profile. For halo profiles which are sharply peaked, MAGIC and HESS are sensitive to neutralino masses above  $\sim 100$  GeV and VERITAS to masses above  $\sim 1$  TeV. Since the diffuse  $\gamma$ -ray background falls with energy, experimental sensitivities improve at high energies, making the high mass higgsino- and wino-dominated neutralinos more easily observable. Future experiments should be able to see the  $\gamma$ -line signal for a wide range of the available parameter space and halo profiles. This could provide not only a discovery of the dark matter particle, but also a measurement of its mass.

Decays of gravitinos can produce an additional, non-thermal abundance of LSPs in Split SUSY [4], which we have not included in our calculations. We expect this to increase the relic abundance and thus change slightly the allowed regions of parameter space from that shown in Fig. 1. In general, this will increase the number density and decrease the mass of the LSP, leading to enhanced indirect signals compared to those presented above.

These indirect dark matter searches tend to complement accelerator and direct detection experiments. Of course, indirect signals can at best provide a detection of the dark matter particle and a measurement of its mass. In order to discover supersymmetry or distinguish Split Supersymmetry from other supersymmetric models, further evidence will be required for example from colliders [27], cosmic ray observatories [28], or neutrino telescopes. A lower mass LSP will be discovered at the LHC, while a heavier one gives the best annihilation signals. Pure higgsino or wino dark matter would be very difficult for direct detection and collider searches [6], but should be detectable indirectly. In this case, astrophysics can fill in the pieces of the puzzle that other experiments have missed.

## Acknowledgements

We would like to thank T. Abel, E.A. Baltz, P. Michelson, and S. Thomas for useful discussions. Special thanks to C. Davis, S. Dimopoulos, A. Pierce, and J.G. Wacker for all their help. P.W.G. is supported by the National Defense Science and Engineering Graduate Fellowship.

## References

- [1] S. Dimopoulos and H. Georgi, Nucl. Phys. B **193**, 150 (1981).
- [2] N. Arkani-Hamed and S. Dimopoulos, arXiv:hep-th/0405159.
- [3] G. F. Giudice and A. Romanino, Nucl. Phys. B **699**, 65 (2004) [arXiv:hep-ph/0406088].
- [4] N. Arkani-Hamed, S. Dimopoulos, G. F. Giudice and A. Romanino, arXiv:hep-ph/0409232.
- [5] B. W. Lee and S. Weinberg, Phys. Rev. Lett. **39**, 165 (1977).
- [6] A. Pierce, Phys. Rev. D **70**, 075006 (2004) [arXiv:hep-ph/0406144].
- [7] L. Bergstrom and P. Ullio, Nucl. Phys. B **504**, 27 (1997) [arXiv:hep-ph/9706232]. P. Ullio and L. Bergstrom, Phys. Rev. D **57**, 1962 (1998) [arXiv:hep-ph/9707333].

- [8] A. Arvanitaki, C. Davis, P. W. Graham and J. G. Wacker, arXiv:hep-ph/0406034.
- [9] M. Binger, arXiv:hep-ph/0408240.
- [10] P. Gondolo, J. Edsjo, P. Ullio, L. Bergstrom, M. Schelke and E. A. Baltz, JCAP **0407**, 008 (2004) [arXiv:astro-ph/0406204]. J. Edsjo and P. Gondolo, Phys. Rev. D **56**, 1879 (1997) [arXiv:hep-ph/9704361]. J. Edsjo, M. Schelke, P. Ullio and P. Gondolo, JCAP **0304**, 001 (2003) [arXiv:hep-ph/0301106]. P. Gondolo and G. Gelmini, Nucl. Phys. B **360**, 145 (1991).
- [11] W. Y. Keung and W. J. Marciano, Phys. Rev. D **30**, R248 (1984).
- [12] A. Burkert, IAU Symp. **171**, 175 (1996) [Astrophys. J. **447**, L25 (1995)] [arXiv:astro-ph/9504041].
- [13] J. F. Navarro, C. S. Frenk and S. D. M. White, Astrophys. J. **490**, 493 (1997).
- [14] C. L. Bennett *et al.*, Astrophys. J. Suppl. **148**, 1 (2003) [arXiv:astro-ph/0302207]; D. N. Spergel *et al.* [WMAP Collaboration], Astrophys. J. Suppl. **148**, 175 (2003) [arXiv:astro-ph/0302209].
- [15] A. Morselli, *Prepared for 8th International Conference on Advanced Technology and Particle Physics (ICATPP 2003): Astroparticle, Particle, Space Physics, Detectors and Medical Physics Applications, Como, Italy, 6-10 Oct 2003*
- [16] F. A. Aharonian, W. Hofmann, A. K. Konopelko, H. J. Volk, Astroparticle Physics **6**, 365 (1997).
- [17] N. Magnussen, arXiv:astro-ph/9805184. V. V. Vassiliev, Astropart. Phys. **11**, 247 (1999) [arXiv:astro-ph/9905044]. J. A. Hinton [The HESS Collaboration], New Astron. Rev. **48**, 331 (2004) [arXiv:astro-ph/0403052].
- [18] L. Bergstrom, P. Ullio and J. H. Buckley, Astropart. Phys. **9**, 137 (1998) [arXiv:astro-ph/9712318].
- [19] D. Hooper and L. T. Wang, Phys. Rev. D **69**, 035001 (2004) [arXiv:hep-ph/0309036].
- [20] P. Ullio, JHEP **0106**, 053 (2001) [arXiv:hep-ph/0105052].
- [21] S. Profumo and P. Ullio, JCAP **0407**, 006 (2004) [arXiv:hep-ph/0406018].
- [22] J. L. Feng, K. T. Matchev and F. Wilczek, Phys. Rev. D **63**, 045024 (2001) [arXiv:astro-ph/0008115].
- [23] M. Boezio *et al.* [WIZARD Collaboration], Astrophys. J. **487**, 415 (1997).
- [24] S. Orito *et al.* [BESS Collaboration], Phys. Rev. Lett. **84**, 1078 (2000) [arXiv:astro-ph/9906426].
- [25] M. A. DuVernois *et al.*, Astrophys. J. **559**, 296 (2001); C. Grimani *et al.*, Astron. & Astrophys. **392**, 287 (2002); M. Boezio *et al.* [WIZARD Collaboration], Astrophys. J. **532**, 653 (2000).
- [26] A. W. Strong, I. V. Moskalenko and O. Reimer, Astrophys. J. **613**, 962 (2004) [arXiv:astro-ph/0406254].
- [27] S. h. Zhu, Phys. Lett. B **604**, 207 (2004) [arXiv:hep-ph/0407072]. W. Kilian, T. Plehn, P. Richardson and E. Schmidt, Eur. Phys. J. C **39**, 229 (2005) [arXiv:hep-ph/0408088]. J. L. Hewett, B. Lillie, M. Masip and T. G. Rizzo, JHEP **0409**, 070 (2004) [arXiv:hep-ph/0408248]. K. Cheung and W. Y. Keung, Phys. Rev. D **71**, 015015 (2005) [arXiv:hep-ph/0408335].
- [28] L. Anchordoqui, H. Goldberg and C. Nunez, Phys. Rev. D **71**, 065014 (2005) [arXiv:hep-ph/0408284].